JOURNAL OF MATERIALS SCIENCE **34** (1999) 6107–6114

Liquid phase sintering of Re_2O_3 YSZ ceramics:

Part II *Grain boundary electrical properties*

M. F. DE SOUZA
Department of Physics and Materials Science, S. Paulo University, P.O. Box 369, 13 560-970 S. Carlos-SP, Brazil
E-mail: mfs@ifsc.sc.usp.br

D. P. F. DE SOUZA
Department of Materials Engineering, Federal University of S. Carlos, P.O. Box 676, 13 565-905 S. Carlos-SP, Brazil
E-mail: dulcina@power.ufscar.br

Grain boundary electrical properties of Y_2O_3 stabilised zirconia with small additions of Er_2O_3 and Pr_2O_3 sintered via silicate liquid phase were studied by the impedance spectroscopy technique. Grain boundary specific conductivity of the praseodymium doped samples was found to be independent of sintering time, while the erbium doped sample showed high anomalous conductivity for the 1.0 h sintered samples. The electrical behaviour is explained considering the grain boundary to be a series association of the glass film and the space charge region. Specific conductivity and Debye length of the space charge region of erbium doped samples were found to be 6.7×10^{-8} S/cm and 0.25 nm, respectively.

1. Introduction

This paper deals with the study of grain boundary electrical conductivity of YSZ-Re_2O_3 ceramic discs sintered via silicate liquid phase, as described in Part I of this paper. The excessive liquid phase and rare earth ions result in unusual electrical behaviour in the grain boundary.

Silica is frequently found associated with zirconia ceramics, causing a deleterious effect on their grain boundary electrical properties, even in very low concentrations [1, 2]. Siliceous phases are normally found in the triple junctions and pockets along the grain boundary. In the past, several studies were done aimed at the effect of the impurities on grain boundary conductivity [3–5]. More recently, Gödickmeier *et al.* [6] studied the effect of intergranular films by the addition of silica and alumina on the grain boundary electrical conductivity of 3Y-TZP ceramics. Clarke [7] theoretically studied the equilibrium thickness of these intergranular glass films and concluded that they are close to 2.0 nm. All the studies done in the past have shown that silica glass films always decrease grain boundary electrical conductivity.

The grain boundary conductivity of high purity YTZ ceramics has been studied by Vekerk *et al.* [8]. Their results have shown that specific grain boundary is still low when compared to grain conductivity. The space charge concept originally introduced by Frenkel [9] and later developed by Kliewer and Koehler [10], and Yan *et al.* [11] has been applied by several authors [12–16] to explain the interface electrical properties of several ceramic systems. Vacancy depletion in the space charge region may be the cause of the grain boundary resistivity of high purity systems such as that studied by Verkerk *et al.* [8].

The results of the grain boundary electrical conductivity of this study are discussed considering the "electric grain boundary" as being a series association of a glass film and the space charge region of the neighbouring grains.

2. Procedure

2.1. Experimental

Ceramic discs for electrical measurements were prepared as described in Part I of this paper. Discs were pressed from powders of eight batches, two for each of the YPr, YPrEr, YY, and YEr compositions that are shown in Table I. These discs were used to perform the work of Part I and present study. Thus, all the electrical measurements of this study were done on discs prepared from the same powders and following the same procedures of cold isostatic pressing and sintering at 1610 °C in air. The discs were polished with a diamond paste with a final grit of 3.0 μm. Platinum electrodes were applied by painting with platinum paint (Demetron 308 A, Germany) and heat treated for 1/2 h at 1000 °C in air. Disc conductivity, capacitance and relaxation time were measured by the impedance spectroscopy technique in the range of 5 Hz to 13 MHz with an impedance analyser (HP 4192 A LF, USA). Measurements were taken in the temperature range of 350–550 °C, with stability better than 3 °C.

TABLE I Nominal samples compositions (mol %)

	Y_2O_3	Pr_2O_3	Er_2O_3
YEr	6.5	—	0.5
YPr	6.5	0.5	—
YPrEr	6.5	0.5	0.5
YY	7.0	—	—

In addition each composition has: $0.5Al_2O_3$, $0.12TiO_2$; 0.12CaO; $2.5SiO_2$ (mol %).

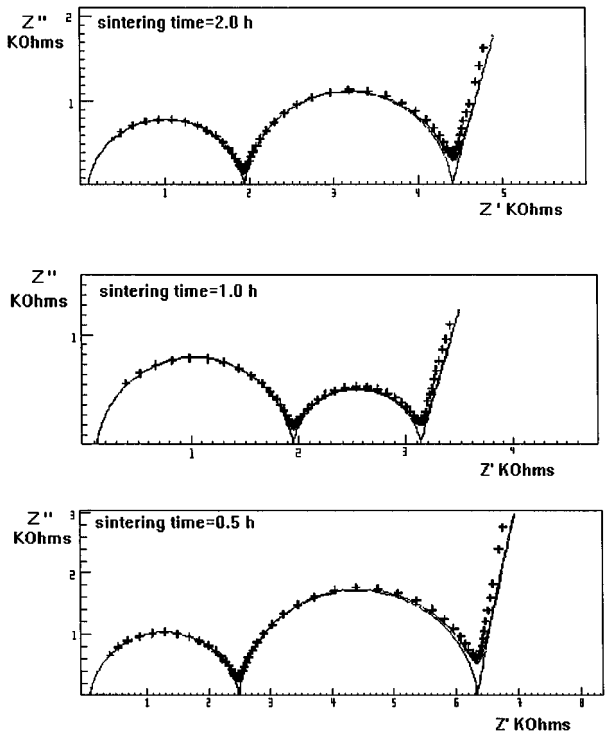

Figure 1 Cole-Cole plots, imaginary part (Z″) vs. real part (Z′) of the impedance, measured at 400 °C of YEr sample.

2.2. Complex impedance analysis

The experimental results of the imaginary part (Z″) of the impedance spectra, plotted against the real part (Z′) of the impedance, measured in the 350–550 °C range, show well defined arcs for the grain and grain boundary impedance of the ceramic discs, Fig. 1. These experimental results will be introduced through the well known quantities R_g, R_{gb}, C_g, and C_{gb}, the grain and grain boundary resistance and capacitance, respectively, obtained directly from the impedance measurements after analysis of the Cole-Cole plots. The macroscopic grain, σ_g, and grain boundary, σ_{gb}, electrical conductivities as well as the normalised capacitance, c_{gb}, were obtained as follows [1, 6]:

$$\sigma_g = L/R_g S \tag{1}$$

$$\sigma_{gb} = L/R_{gb} S \tag{2}$$

$$c_{gb} = C_{gb} L/S \tag{3}$$

where S and L are the electrode area and the thickness of the ceramic discs, respectively. The above quantities are macroscopic quantities in the sense that they are the combination of the elementary resistors and capacitors that make the sample from the electrical point of view. Let us consider the microscopic grain boundary quantities, specific conductivity, dielectric constant, and thickness of the grain boundaries. The electrical contact between two grains is made through the grain boundary material that can be represented locally by a resistance, r_i, and a capacitance, c_i, in a parallel arrangement. The grain boundary sample resistance, R_{gb}, is a combination of all r_i that is dependent on their peculiar arrangement inside the solid. The same can be said for C_{gb} because both are extensive quantities. The relaxation time, τ, of each of these r_i and c_i pairs, is an intensive quantity, given by $\tau_i = r_i \times c_i$, that can be expressed by:

$$\begin{aligned}\tau_i = r_i \times c_i &= \left(\rho_{gb}^{sp}\delta_{gb}/\alpha\right) \times \left(\varepsilon_o \varepsilon_{gb}\alpha/\delta_{gb}\right) \\ &= \rho_{gb}^{sp}\varepsilon_o\varepsilon_{gb} = \varepsilon_o\varepsilon_{gb}/\sigma_{gb}^{sp}\end{aligned} \tag{4}$$

where ρ_{gb}^{sp}, ε_{gb}, and σ_{gb}^{sp} are, respectively, the specific resistivity, dielectric constant and specific conductivity of the grain boundary material, ε_o the electric permittivity of vacuum, δ_{gb} the thickness of the grain boundary and α the area of part of the grain boundary considered. If the grain boundary material is uniform, the relaxation time of the whole sample will be the same as that of the elementary capacitors and resistors, regardless of the model used to relate the microscopic with the macroscopic quantities. Therefore:

$$\tau/\varepsilon_o = R_{gb}C_{gb}/\varepsilon_o = \varepsilon_{gb}/\sigma_{gb}^{sp} = \tau_i/\varepsilon_o \tag{5}$$

This result allows for measurement of the ratio of specific quantities of the grain boundary, conductivity and dielectric constant, regardless of the model used to correlate microscopic with macroscopic quantities. This is true even in a system where large amounts of glass are in the grain boundaries, like the systems we are studying. The degree of uniformity of the grain boundary material can be estimated by how much the corresponding Cole-Cole plot deviates from a semicircle [17].

Although the percolation model would more adequately represent the system studied, it lacks an analytical representation. A simple model, such as the "brick layer model", is needed to calculate σ_{gb} and c_{gb} from the specific quantities, as has already been done by other authors [1, 6] using Equations 6 and 7

$$\sigma_{gb} = \sigma_{gb}^{sp}\, d_g/\delta_{gb} \tag{6}$$

$$c_{gb} = \varepsilon_o\varepsilon_{gb} d_g/\delta_{gb} \tag{7}$$

According to these equations, the σ_{gb}/d_g ratio will be constant if σ_{gb}^{sp} and δ_{gb} are constants. Moreover, the c_{gb}/d_g ratio will be constant if ε_{gb} and δ_{gb} are constants. Later in this paper, a correction to Equations 6 and 7 will be discussed to aid interpretation of the σ_{gb} and c_{gb} data.

3. Results

The grain conductivity, σ_g, divides the studied discs into two groups: that of the YEr and YY samples with higher conductivity and the group of YPr and YPrEr sample

TABLE II Conductivity activation energies (eV)

	YPr			YEr			YY			
Grain boundary conductivity										
Sintering time (h)	0.5	1.0	16.0	0.5	1.0	16.0	0.5	1.0	8.0	16.0
Activation energy (eV)	1.09	1.10	1.09	1.08	1.03	1.08	1.09	1.09	1.08	1.08
Specific grain boundary conductivity/ε_{gb}										
Sintering time (h)	5	1.0	16.0	5	1.0	16.0	0.5	1.0	8.0	16.0
Activation energy (eV)	1.11	1.11	1.11	1.12	1.05	1.11	1.10	1.10	1.08	1.08

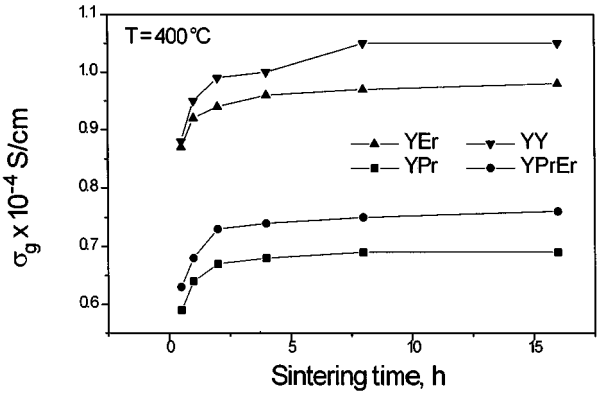

Figure 2 Grain conductivity, measured at 400 °C, vs. sintering time.

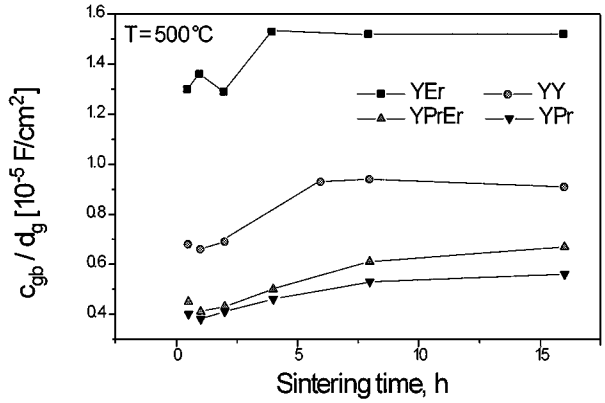

Figure 4 Reduced capacitance over the grain size, c_{gb}/d_g, measured at 500 °C, vs. sintering time, t_s.

discs, whose conductivity values are around 40% lower as shown in Fig. 2. Conductivity grows in the first hours of sintering in the case of each sample composition. Activation energy for the grain conductivity was found to be $1.06 \pm 0{,}02$ eV from 350 to 550 °C for all samples.

The ratio of the grain boundary electrical conductivity and grain size, σ_{gb}/d_g, and the ratio of the normalised capacitance and grain size, c_{gb}/d_g, dependence with sintering time are shown in Figs 3 and 4, respectively. If the intensive quantities, σ_{gb}^{sp} and ε_{gb} as well as δ_{gb} are constants, according to Equations 6 and 7 these ratios should be time independent. The activation energies σ_{gb}, Fig. 5, range from 1.11 to $1.08 \pm 0,02$ eV. The YEr 1.0 h and the YY 8.0 h sintered discs show activation energies of 1.03 and 1.08 ± 0.01 eV, respectively (see Table II). Growth of the σ_{gb}/d_g ratio with sintering time is larger for the YPrEr and YPr samples and smaller for the YEr sample. The YEr 1.0 h sintered sample discs have, as shown in Fig. 3, the σ_{gb}/d_g ratio $\approx$2.5 times higher than expected from the dependence

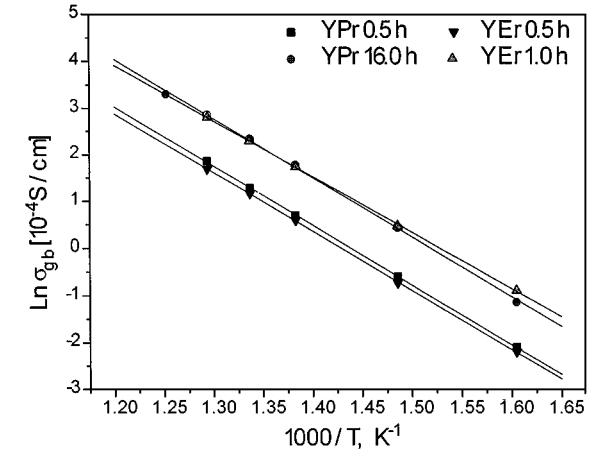

Figure 5 Arrhenius plot of the grain boundary conductivity. See also Table II for the activation energies.

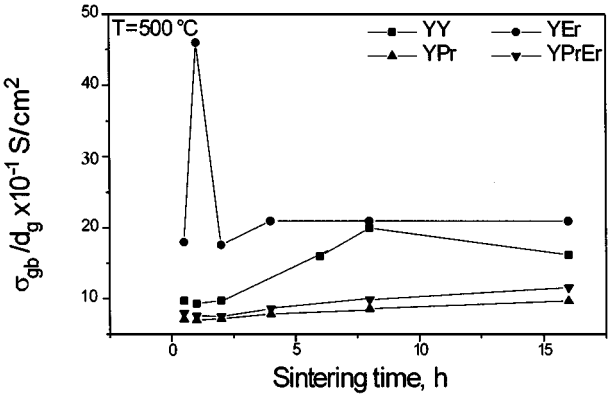

Figure 3 Grain boundary conductivity over the grain size, σ_{gb}/d_g, measured at 500 °C, vs. sintering time, t_s.

of σ_{gb} with d_g from Equation 6. The c_{gb}/d_g ratio does not show this same high anomalous increase as shown in Fig. 4. The 8.0 h sintered discs of the YY sample also show an anomalous dependence of σ_{gb}/d_g with sintering time, albeit less pronounced, as shown in Fig. 3.

The above results show the behaviour of the extensive macroscopic electrical properties with sintering time. Let us now observe the behaviour of the intensive variables that are directly connected with the material properties, as already previously discussed. We chose to represent the intensive variables with the ε_o/τ_{gb} ratio. From Equation 5 this ratio is $\varepsilon_o/\tau_{gb} = \sigma_{gb}^{sp}/\varepsilon_{gb}$. The ε_o/τ_{gb} ratio has the following characteristics for each sample. The YPr and YPrEr samples show the ε_o/τ_{gb} ratio is soaking time independent and increases with the measuring temperature, with activation energy slightly higher than that of σ_{gb}, see Fig. 6, Fig. 7 and Table II.

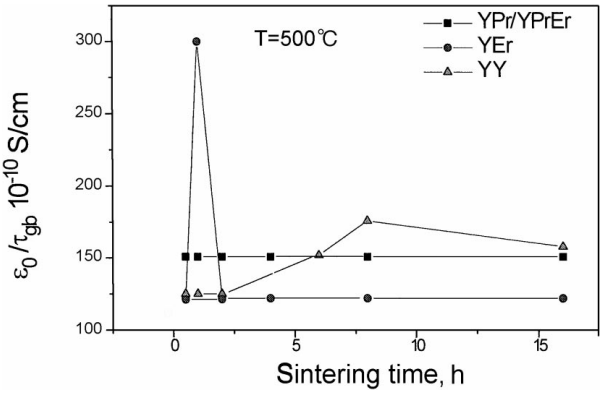

Figure 6 Vacuum permitivity over the grain boundary relaxation time, ε_o/τ_{gb}, vs. sintering time, t_s.

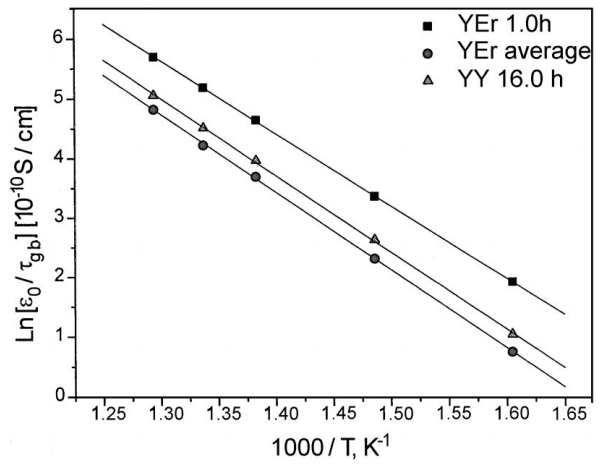

Figure 7 Vacuum permitivity over the grain boundary relaxation time $\varepsilon_o/\tau_{gb} = \sigma_{gb}/\varepsilon_{gb}$.

For the YEr 1.0 h sintered discs the same $\varepsilon_o/\varepsilon_{gb}$ ratio is 2.5 times larger than for other sintering times, following the same behaviour of σ_{gb}. The activation energies are the same for the discs of YEr composition, while for σ_{gb}, the 1.0 sintered disc has a lower activation energy, 1.05 ± 0.01 eV. The ε_o/τ_{gb} for the YY samples changes with the sintering time, showing a maximum at 8.0 h of sintering as shown in Fig. 6.

The c_{gb}/d_g ratio, Fig. 4, scales with σ_{gb}/d_g in order to produce the respective ε_o/τ_{gb} ratio of each disc. Note that the anomalous growth of σ_{gb}, as well of ε_o/τ, of the YEr 1.0 h sintered discs is not followed by an appreciable growth in the grain boundary capacitance. Therefore, according to Equations 5–7, the anomalous growth in σ_{gb} is entirely attributable to the σ_{gb}^{sp} increase. This result means that the anomalous increase of the grain boundary conductivity is due to a large change in material electrical conductivity and a very small variation in grain boundary capacitance.

4. Discussion

4.1. Grain conductivity

Rare earth additions have a clear influence on σ_g grain conductivities. The YY and YEr sample grains are 25% more conductive in relative to the YPr and YPrEr samples, as shown in Fig. 2. The total stabilising ion concentration between the two pairs of compositions differ by ≈0.3 mol %, (see Table II, Part I). The effect of the ionic radius on grain conductivity was studied by Stafford *et al*. [18], who found neodymium ion doped zirconia is 5 times less conductive than the Y_2O_3 stabilised zirconia, both with the same molar concentration. The difference in grain conductivity between the samples of this study can be understood considering that 4.6% of the Y^{+3} ion was substituted by the Pr^{+3} ion, of nearly the same ionic radius as the Nd^{+3} ion. Assuming that the effect of the ionic radius misfit on σ_g is linear with concentration, the calculated conductivity decrease of the praseodymium doped samples is 23% smaller than the yttrium doped one. This is quite close to the observed 25% difference.

The conductivity increased with sintering time shows almost the same behaviour for all samples, irrespective of their grain size. In the first 1/2 h of sintering the conductivities have attained nearly 85% of their final values and after 4.0 h of sintering they maintain a constant value. YY samples show slightly higher conductivity for the 8.0 h sintered samples. The conductivity increased with sintering time indicates that, due to the fast rate of grain growth, the grains are not in equilibrium with the liquid phase. The effect of porosity on conductivity must be discarded because the micrographs showed very few pores in the grains. Although further experiments are needed to clarify the effect of fast grain growth on grain conductivity, the following experiment was made. The EDS analysis of the liquid phase of the YEr sample of the present work found the presence of erbium in the liquid phase in the first 4.0 h of sintering, while at higher sintering times it was not detected. From this observation we may conclude that in the first 4.0 h of sintering the concentration of stabilising ions in the liquid phase is above its equilibrium concentration. Therefore, up to the first 1/2 h of sintering, the grains would have incorporated a lower concentration of stabilising ions, but this concentration increases progressively, following the decreased rate of grain growth, in order to establish the thermodynamic equilibrium between both phases.

4.2. Grain boundary

This section discusses grain boundary electrical properties, while the anomalous conductivity behaviour of the YEr 1.0 h and YY 8.0 h sintered samples will be discussed in the next section. Usually, quantities such as σ_{gb}^{sp}, ε_{gb}, and δ_{gb} are obtained from the quantities σ_{gb}, c_{gb} and additional data, e.g., grain boundary thickness, are obtained through high-resolution electron microscopy, with the help of a model that relates these quantities, such as the brick layer model [6 ,8]. In this model, the grain boundary is represented by layers of equal thickness and the same area of the electrodes, *S*, normal to the current flow. To represent the grain boundary of the samples of this study, where only a part of the grain boundary is conductive, the best approach would be to use a percolation model (see Fig. 1a, Part I). However, this model lacks an analytical representation for the extensive quantities, which makes it difficult to use. Another much simpler approach is to consider the model represented in Fig. 8, where *A* is the total

TABLE III $\delta_{gb}S/A$ (nm)[a] dependence with sintering time at 500 °C and $\varepsilon_{gb} = 30$

	YEr		YprEr				YPr		YY	
Sintering time (h)	$\delta_{gb}S/A$ (nm)	$A/A_{0.5\,h}$ [b]	$\delta_{gb}S/A$ (nm)	$A/A_{0.5\,h}$	A/S	δ_{gb} (nm)	$\delta_{gb}S/A$ (nm)	$A/A_{0.5\,h}$	$\delta_{gb}S/A$ (nm)	$A/A_{0.5\,h}$
0.5	2.04	1.00	5.9	1.00	0.36	2.1	6.6	1.00	3.9	1.00
1.0	1.95	1.05	6.5	0.91	0.33	2.1	7.0	0.94	4.0	0.97
2.0	2.06	0.99	6.2	0.95	0.34	2.1	6.5	1.01	3.9	1.00
4.0	1.74	1.17	5.3	1.11	0.40	2.1	5.8	1.14	—	—
6.0	—	—	—	—	—	—	—	—	2.9	1.34
8.0	1.75	1.16	4.3	1.37	0.49	2.0	5.0	1.32	2.8	1.39
16.0	1.75	1.16	4.0	1.47	0.53	2.1	4.7	1.40	2.9	1.34

[a]Calculated using Equation 8.
[b]Relative growth of the contact area.

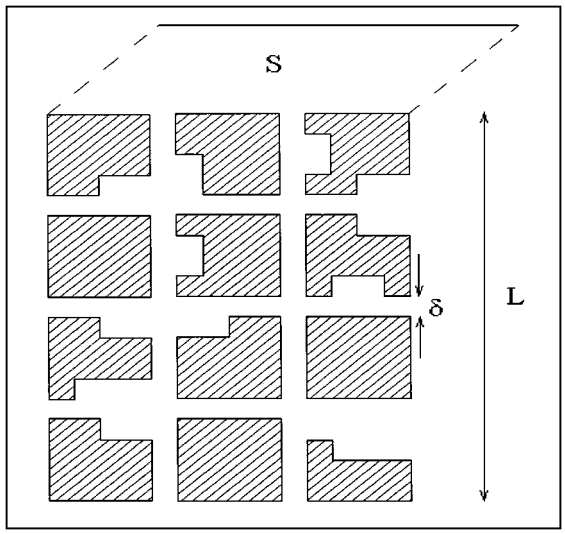

Figure 8 Modified "brick-layer" model. S—disc area; L—disc thickness; δ—thickness of thinner regions of the grain boundary.

effective conducting area normal to the current flow, δ_{gb} is the grain boundary thickness, and S is the electrode area. Introducing the fractional conducting area, A/S, the following modifications in Equations 5–7 should be made. Equation 5 does not change, while Equations 6 and 7 become, respectively,

$$\sigma_{gb} = \sigma_{gb}^{sp} d_g A / \delta_{gb} S \tag{8}$$

$$c_{gb} = \varepsilon_o \varepsilon_{gb} d_g A / \delta_{gb} S \tag{9}$$

Equation 5 is valid even in a percolation model because it refers to the intensive quantities of the ceramic disc. If the conductivity or the dielectric constant changes according to position, then the corresponding Cole-Cole plot is no longer a perfect semicircle. Modelling on a large electric circuit, a variation of 2% on τ was measured by doubling the relaxation time of 2% of the individual $r_i c_i$ pairs. For this reason, we will take Equation 5 as being suitable to express our results in the following form:

$$\sigma_{gb}^{sp} / \varepsilon_{gb} = \varepsilon_o / \tau_{gb} \tag{10}$$

We take, for the macroscopic dielectric constant, $\varepsilon_{gb} = 30$, a choice that produces δ_{gb} values around 2.0 nm through Equation 9, as is shown in Table III. The c_{gb}/d_{gb} ratio should be independent of the sintering time, according to Equation 9, if the dielectric constant, ε_{gb}, and the A/S ratio were constant, taken δ_{gb} constant, as has already been assumed. The dielectric constant was chosen to be constant because the relaxation time does not correlate with the capacitance increase. Thus, the increase in the c_{gb}/d_g ratio with the sintering time is due to the increase of the A/S ratio. The A/S ratio of YPrEr 8.0 h sintered discs was evaluated from Fig. 1 of Part I at 0.5. It was considered that the average A_i/S ratio is equal to A/S. This result, together with the relative variation of A, was used to calculate the A/S values for the other sintering times, as shown on Table III. These A/S values are a rough estimate but indicate that if $\varepsilon_{gb} = 30$, the electrical grain boundary thickness is close to 2.0 nm. The A/S values for the YEr samples are higher than those of the YPrEr because of their smaller grain size, giving δ_{gb} values slightly smaller than 2.0 nm.

TABLE IV Specific grain boundary conductivity, σ_{gb}^{sp}, at 500 °C

Ceramics	$\sigma_{gb}^{sp} \times 10^{-8}$ (S/cm)	Observations
YEr (1.0 h)	90.0	This work ($\varepsilon_{gb} = 30$)
YEr (average)	36.6	
YPr/YprEr (average)	45.0	
YY (low)	37.0	
YY (high 8.0 h)	47.0	
15 mol % CaO (FSZ)	3.8	Ref. [1] high purity ZrO_2 ($d_g = 12\ \mu m$)
10 mol % Y_2O_3 (FSZ)	15.7	Ref. [2] high purity ZrO_2 ($d_g = 12\ \mu m$)
7 mol % Y_2O_3 (FSZ)	58.0	Recalculated from Ref. [8] ($d_g = 12\ \mu m$) and ($\varepsilon_{gb} = 30$)

The specific grain boundary conductivities can now be calculated using Equation 10, the above discussed value of the dielectric constant, $\varepsilon_{gb} = 30$, and the experimental ε_o/τ_{gb} data shown in Fig. 6. Table IV compares the σ_{gb}^{sp} of the samples of this work with literature values, recalculated to be close to the grain size and dielectric constant of our data. The highest values of the specific grain boundary conductivity, shown in Table IV, refer to the YEr 1.0 h sintered sample and the high purity sol-gel processed sample of Verkerk *et al.* [8] The high purity sample of Badwal and Drennan [2], where a small amount of second phase was found, has specific

grain boundary conductivity close to the YPrEr sample discs. The dependence of grain boundary conductivity on sintering time follows the same general behaviour of c_{gb}, as expected from Equations 8 and 9.

Activation energies for σ_{gb} and σ_{gb}^{sp} are shown in Table II. Although the difference between them is small, the activation energies for σ_{gb} are systematically lower than those of σ_{gb}^{sp}. The YEr 1.0 h sintered discs also show activation energies smaller than those of other samples. The increase of the activation energies of $\sigma_{gb}^{sp}/\varepsilon_{gb}$ relative to σ_{gb} can be accounted for if the grain boundary thickness, δ_{gb}, increases with the temperature, Equation 8. An increase of about 4% in δ_{gb}, in the measuring temperature range, is sufficient to account for the difference in the activation energies between σ_{gb} and σ_{gb}^{sp}.

The dependence of $\sigma_{gb}^{sp}/\varepsilon_{gb}$ with the sintering time, Fig. 6, shows that specific grain boundary electrical properties has a high degree of constancy for each composition during the entire sintering process, being grain size independent. Significant changes were observed simultaneously with the anomalous increase in σ_{gb}. For the YPr and YPrEr sample discs the degree of constancy of τ_{gb}, measured at 500 °C for each sintering time (average values shown in Fig. 6), has a deviation of around 5% that is attributed to temperature instability during measurements.

In this section a model is proposed to understand the results of conductivity. First, it was considered that grain boundary electrical conduction is done, preferentially, through the thinner regions. It has been assumed that the glass phase present in these thinner regions is squeezed to ≈2.0 nm thickness, as proposed by Clarke [7]. The consequence of this choice allocates to the dielectric constant, $\varepsilon_{gb} = 30$, a value between the bulk dielectric constant of zirconia and that of the glass film. To take into account the uneven structure of the grain boundary, in order to use the brick layer model approximation, the authors introduced the fractional contact area between the grains, which was found to increase with sintering time. The slightly higher activation energies of the specific grain boundary conductivity can be attributed to the increase of grain boundary thickness, δ_{gb}, with the increase in measuring temperature. The constancy of the grain boundary relaxation time throughout the sintering time suggests constancy of the electrical properties of the grain boundary material and will be discussed in the next section.

4.3. Anomalous conductivity behaviour

Let us consider the conducting grain boundary as consisting of a thin glass film squeezed between two ceramic grains, each grain with its space charge region as shown in Fig. 9, where "gl" refers to the glass phase film and "sc" to the space charge regions. If the space charge, as well the nature of the glass film, do not change with the sintering time, the relaxation time, τ_{gb}, will be constant. This means that the resistance per unit area of the glass film and that of the space charge, R_{gl} and R_{sc}, respectively, as well the capacitance per unit area, C, remain constant throughout the sintering time. This

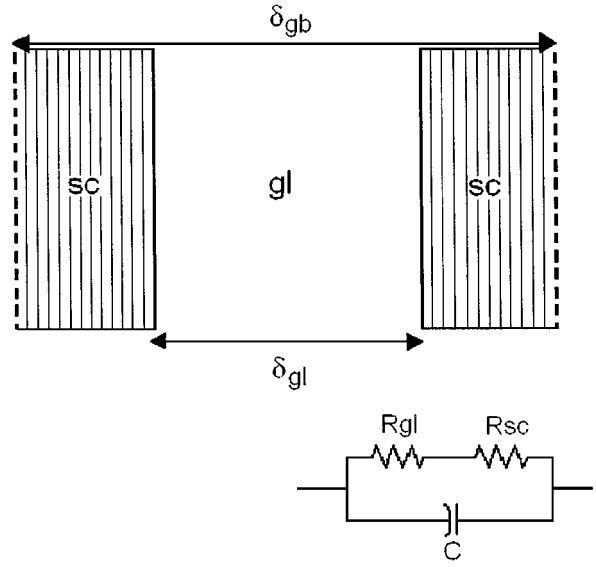

Figure 9 Model of the thinner regions of the grain boundary: gl = glass film; sc = space charge region of each grain in contact with the glass film; δ_{gl} = glass film thickness; δ_{gb} = total grain boundary electrical thickness; C, R_{gl}, and R_{sc} are, respectively, the capacitance per unity area, glass film resistance per unity area and space charge resistance per unity area.

describes well the electrical behaviour of the YPr and YPrEr samples characterised by a constant relaxation time. Moreover, it is also considered that a large increase in the glass conductivity cannot occur because these glasses lack a source of charge carriers, such as the alkali ions. Hence, R_{gl} will be considered constant or having small variations among samples. The YPr and the YPrEr samples also have a constant value for R_{sc}. According to the space charge model of ceramic interfaces [9, 16], these two samples should have a depleted vacancy concentration in the space charge region, corresponding to an enrichment of the grain surface with trivalent ions, in this case Pr^{+3} ions. This means that the segregation of the Praseodymium must be high, as was proven experimentally (see Table IV Part I). It should be noted that the segregation coefficient of the Y^{+3}, the majority stabilising ion, is close to 1.0 and, therefore, the build-up of the space charge must have a large contribution of the Pr^{+3} ions in the YPr and YPrEr samples. This does not apply to the YY and YEr samples, where only the low concentration ions like Ca^{+2} are segregated. The large increase in σ_{gb} of the YEr 1.0 h sintered sample is followed by a corresponding jump in σ_{gb}^{sp}. The capacitance also increases, although only to a very small extent, ≈7.0%, Fig. 4. The measured capacitance, C in Fig. 9, is the series association of the glass phase capacitance, C_{gl}, with the space charge capacitance, C_{sc}. It is assumed that C_{sc} is larger than C_{gl} because the dielectric constant of the ceramic grains is higher than that of the glass phase and the thickness of the glass phase is expected to be larger than the Debye length of the space charge, $C_{sc} > C_{gl}$. Assuming values for the dielectric constant of the space charge and the glass phase of 50 and 15, respectively, the Debye length of the space charge can be calculated from the experimentally observed 7.0% capacitance variation, considering the following. For sintering times during

and after the conductivity increase, the capacitance of the space charge, C_{sc}, and glass film, C_{gl}, are given by:

$$C_{sc} = \varepsilon_o \varepsilon_{sc} A_i / \delta_{sc} \quad (11)$$

$$C_{gl} = \varepsilon_o \varepsilon_{gl} A_i / \delta_{gl} \quad (12)$$

In the above expressions ε_{sc} and ε_{gl} are the dielectric constant of the space charge and the glass film, respectively, δ_{sc} the Debye length of the space charge and ε_{gl} the glass film thickness that we have already assumed to be 2.0 nm. The values for the dielectric constants ε_{sc} and ε_{gl} were chosen in the following way. The ε_{gl} was taken from reference [6]. The ε_{sc} now refers to the zirconia grains dielectric constant, while the grain boundary dielectric constant, ε_{gb}, is a combination of ε_{gl} and ε_{sc}. Assuming that during the increase in conductivity the Debye length becomes very small, in order to decrease the grain boundary resistance, the series capacitance, C, becomes

$$C = C_{gl} \quad (13)$$

From the Equations 11 to 13 is possible to calculate the space charge Debye length, that is found to be 0.25 nm.

Let us now consider the grain boundary resistance per unit area, see Fig. 9, during and after the conductivity increase.

$$R'_{gb} = \rho_{gl}^{sp} \delta_{gl} \quad (14)$$

$$R''_{gb} = \rho_{gl}^{sp} \delta_{gb} + \rho_{sc}^{sp} \delta_{sc} \quad (15)$$

Where R'_{gb} and R''_{gb} are the grain boundary resistance per unit areas during and after the conductivity increase, respectively. ρ_{gl}^{sp} and ρ_{sc}^{sp} are the glass film and space charge specific resistivity, respectively. From Equations 14 and 15 and from the experimental data, the specific conductivity of the glass film and the space charge were calculated and found to be $\sigma_{gl}^{sp} = 6.0 \times 10^{-7}$ S/cm and $\sigma_{sc}^{sp} = 6.7 \times 10^{-8}$ S/cm. The value for σ_{sc}^{sp} compares well with the grain boundary conductivity of very pure boundaries, like the sol-gel samples of Verkerk *et al.* [8]. This comparison should take into account the values of the grain boundary electrical thickness. Our σ_{gb}^{sp} was calculated for a thickness nearly ten times smaller than in the Verkerk *et al.* [8] work. The glass phase conductivity, σ_{gl}, agrees well with the grain boundary conductivity found by Gödickmeier [6] for 3Y-TZP with an intergranular glass film.

The above results, based on the assumption that the glass phase thickness and conductivity were constant during sintering, shows that in fact the specific grain boundary resistivity of Y_2O_3 doped high purity zirconia is due to the depleted vacancy concentration inside the space charge region. These results could be improved if the thickness of the thin glass phase were measured in order to allow for a better estimate of the space charge Debye length. In a recent paper Guo [13] discussed the possibility of improving the grain boundary conductivity. This author considered the introduction of interstitial aluminium trivalent ions in the space charge region as a way to increase the vacancy concentration in the depleted region. This possibility cannot be discarded in this study, but it seems difficult to explain the transient behaviour observed, since Al^{+3} ions were present in all the samples and were strongly segregated. We propose the following tentative explanation for the observed behaviour of the space charge. As mentioned earlier, yttrium ions have a segregation coefficient close to 1.0, that means no segregation, between the glass phase and the zirconia grains. Erbium was not detected in the grain boundary glass after eight hours of sintering. However, Er^{+3} ions were present in the glass phase in the first hours of sintering due to the fast rate of grain growth at that sintering stage. It is also possible that excess Er^{+3} ions migrating from the glass phase to the grain bulk, their preferred location, had disturbed the grain surface charge and therefore temporarily increased the vacancy concentration in the space charge region. Because Yttrium segregation is close to 1.0 the space charge build-up will be dominated by the segregation behaviour of the other stabilising ions, Ca^{+2} and Er^{+3}. These two ions have opposite segregation behaviours, the Ca^{+2} being strongly segregated, like the Pr^{+3} ion in the YPr and YPrEr samples. The process of incorporating Er^{+3} ions stops when the concentration of Er^{+3} in the glass phase becomes small, making the effect of the Ca^{+2} ions dominant. It is emphasised that the important point in the interpretation of these results is the segregation behaviour of most of the stabilising Y^{+3} ions, i.e. close to 1.0. This imparts instability to the system that brings the space charge region from the non-conducting to the conducting state and vice versa. Therefore, small variations in the concentration of the minority ions can produce the anomalous conductivity growth observed. This is a transient process that is due the finite amount of Er^{+3} ions. Preliminary measurements have shown that it lasts around 20 min at 1610 °C.

A similar, though less intense, process occurred in the YY samples for a longer period of time. We tentatively attribute this behaviour also to a temporary disturbance in the space charge. An excess concentration of Y^{+3} ions in the glass phase that wets the grains will increase the diffusion of Y^{+3} ions to the grains. The temporary increase in the Y^{+3} ion concentration may originate in the glass phase separation (see Part I).

5. Conclusions

The electrical properties of the grain boundaries of the four studied compositions have been analysed considering the grain boundary to be made of a glass film and the space charge inside the solid surface in a series association. Grain boundary relaxation time, directly related to specific grain boundary resistivity, was used to study this association. The constant relaxation time of Pr^{+3} doped samples was interpreted as being due to a stable space charge, in the sense that it keeps the vacancy depleted space charge region stable. For those samples, therefore, the Debye length and electrical resistance of the space charge is constant with sintering time. This behaviour was attributed to the strong segregation of Pr^{+3} ion, taking in account that the Y^{+3} ion

has a segregation coefficient close to 1.0. Due to this Y^{+3} ion behaviour and the Er^{+3} ion preference for the grains, the space charge of the YEr and YY samples becomes susceptible to diffusion of these ions to the grains, causing vacancy depletion in the space charge to decrease or be annihilated. This transient effect would eventually be halted by the smaller concentration ions, such as the Ca^{+2} ion, that is strongly rejected. One possible source of extra Y^{+3} ions was attributed to the glass phase separation inside the grain boundaries. Thus, segregation behaviour and glass phase separation disturb the space charge, temporarily decreasing its resistance.

Acknowledgements

The financial support from FAPESP and CNPq are acknowledged.

References

1. M. AOKI, Y. M. CHIANG, I. KOSACKI, L. J. R. LEE, H. TULLER and Y. LIU, *J. Amer. Ceram Soc.* **79** (1996) 1169.
2. S. P. S. BADWAL and J. DRENNAN, *J. Mater. Sci.* **22** (1987) 3231.
3. S. RAJENDRAN, J. DRENNAN and S. P. S. BADWAL, *J. Mater. Sci. Let.* **6** (1987) 1431.
4. M. J. VERKERK, A. J. A. WINNBUST and A. J. BURGGRAAF, *J. Mater. Sci.* **17** (1882) 3113.
5. Y. H. KIM and H. G. KIM, *ibid.* **5** (1994) 260.
6. M. GÖDICKMEIER, B. MICHEL, A. OLIUKAS, P. BOHAC, K. SASAKI, L. GLAUCKER, H. HEINRICH, P. SCHWANDER, G. KOSTORZ, H. HOFMAN and O. FREI, *J. Mater. Res.* **9** (1994) 1228.
7. D. R. CLARKE, *J. Amer. Ceram. Soc*. **70** (1987) 15.
8. M. J. VERKERK, A. J. MIDDELHUIS and A. J. BURGGRAAF, *Solid State Ionics* **6** (1982) 159.
9. J. FRENKEL, "Kinetic Theory of Liquids" (Oxford University Press, New York, 1946) p. 37.
10. K. L. KLIEWER and J. S. KOEHLER, *Phys. Rev.* **140**(4A) (1965) 1226.
11. M. F. YAN, R. M. CANNON and H. K. BOWEN, *J. Phys.* **54** (1983) 779.
12. S. L. HWANG and I. V. CHEN, *J. Amer. Ceram. Soc.* **73** (1990) 3269.
13. X. GUO, *J. Eur. Ceram. Soc.* **16** (1996) 575.
14. A. S. IKEDA and Y. M. CHIANG, *J. Amer. Ceram. Soc.* **76** (1993) 2437.
15. W. D. KINGERY, *ibid.* **57** (1974) 1.
16. S. M. MUKHOPADHYAY and J. M. BLAKELY, *ibid.* **74** (1991) 25.
17. M. KLEITZ, H. BERNARD, E. FERNANDEZ and E. SCHOULER, in "Advances in Ceramics," Vol. 3, edited by A. H. Heuer and L. W. Hobbs (ACerS, 1981) p. 316.
18. R. J. STAFFORD, S. J. ROTHMAN and J. L. ROUTBORT, *Solid State Ionics* **37** (1989) 67.

Received 9 April 1998
and accepted 21 June 1999